Proceedings of the DIS'2004, Štrbské Pleso, Slovakia

TEST OF QCD USING MULTIJETS IN NEUTRAL CURRENT DIS AT HERA

LIANG LI
ON BEHALF OF THE ZEUS COLLABORATION
University Of Wisconsin-Madison
1150 University Avenue, Madison, WI-53706, USA
E-mail: liangli@mail.desy.de

Multijet production rates in neutral current deep inelastic scattering have been measured in the range of exchanged boson virtualities $10 < Q^2 < 5000\,\mathrm{GeV}^2$. The data were taken at the *ep* collider HERA with centre-of-mass energy $\sqrt{s} = 318\,\mathrm{GeV}$ using the ZEUS detector and correspond to an integrated luminosity of $82.2\,\mathrm{pb}^{-1}$. Next-to-leading-order QCD calculations were compared with the data.

1 Introduction

At leading order (LO) in the strong coupling constant, α_s, dijet production in neutral current DIS proceeds via the boson-gluon-fusion (BGF, $V^*g \to q\bar{q}$ with $V = \gamma$, Z^0) and QCD-Compton (QCDC, $V^*q \to qg$) processes. Events with three jets can be seen as dijet processes with an additional gluon radiation or splitting of a gluon into a quark-antiquark pair, and are directly sensitive to $\mathcal{O}(\alpha_s^2)$ QCD effects. The higher sensitivity to α_s and the large number of degrees of freedom of the trijet final state allow the testing of QCD predictions in great detail.

2 Event selection

The data used in this analysis were collected during the 1998-2000 running period, when HERA operated with protons of energy $E_p = 920$ GeV and electrons or positrons of energy $E_e = 27.5$ GeV, and correspond to an integrated luminosity of $82.2 \pm 1.9\ \mathrm{pb}^{-1}$. Neutral current DIS events were selected and the kinematic range of the analysis is defined as:

$$10 < Q^2 < 5000\ \mathrm{Gev}^2 \text{ and } 0.04 < y < 0.6$$

Jets were reconstructed using the k_T cluster algorithm [1] in the longitudinally invariant inclusive mode. The jet search was conducted in the Breit frame [2]. The jet phase-space is defined by selection cuts on the jet pseudorapidity $\eta^{\mathrm{jet}}_{\mathrm{LAB}}$ in the laboratory frame and on the jet transverse energy $E^{\mathrm{jet}}_{T,B}$ in the Breit frame:

$$-1 < \eta^{\mathrm{jet}}_{\mathrm{LAB}} < 2.5 \text{ and } E^{\mathrm{jet}}_{T,B} > 5\ \mathrm{Gev}$$

Events with two (three) or more jets were selected by requiring the invariant mass of the two (three) highest $E^{\mathrm{jet}}_{T,B}$ jets to be:

$$M_{\mathrm{JJ}}(M_{3\mathrm{J}}) > 25\ \mathrm{Gev}$$

These requirements were necessary to ensure a reliable prediction of the cross sections to next-to-leading order.

3 NLO QCD calculations

The NLO calculations were carried out in the $\overline{\mathrm{MS}}$ scheme for five massless quark flavors with the program NLOJET [3] using either CTEQ6 [4], CTEQ4 [5] or MRST2001 [6] proton parton density functions (PDFs). It was checked that the LO and NLO calculations from NLOJET agree with those of DISENT [7] at the 1-2% level for the dijet cross sections when a fixed α_{EM} coupling is used, the renormalisation scale μ_R^2 is set to $(\bar{E}_T^2 + Q^2)/4$, the factorization scale μ_F^2 is set to Q^2 and $\bar{E}_T$ is the average E_T of the two (three) highest E_T jets in a given event for dijets (trijets). For comparison with the data, three above PDFs were used and the renormalisation and factorization scales were both chosen to be $(\bar{E}_T^2 + Q^2)/4$ for best description of the data. The NLO QCD predictions were corrected for hadronisation effects using a bin-by-bin procedure.

4 Results

The differential dijet and trijet cross sections as functions of Q^2 are presented in Fig. 1. The NLO predictions using NLOJET with CTEQ6 PDF, corrected for hadronisation effects using LO MC, are compared to the data. The data is also compared with the NLO predictions using the CTEQ4M and MRST2001 PDF, as shown in Fig. 2. The QCD predictions provide a good description of both the shape and magnitude of the measured cross sections for all three PDFs, even at low Q^2.

Fig. 3 shows the cross-section ratio $R_{3/2}$ of trijet cross section to dijet cross section, as a function of Q^2. The correlated systematic and the renormalisation scale uncertainties cancel in the ratio. The agreement between the data and NLO predictions is good within the substantially reduced uncertainties (experimental $\sim$ 5%, theoretical $\sim$ 7%) compared with uncertainties in dijet and trijet cross sections. A similar comparison of data and the NLO predictions using CTEQ4 PDF is shown in Fig. 4. The NLO calculations of $R_{3/2}$ were performed for five sets of the CTEQ4 "A-series" obtained assuming $\alpha_s(M_Z)$=0.110, 0.113, 0.116, 0.119, 0.122, respectively. The NLO predictions are sensitive to $\alpha_s(M_Z)$ values, thus encourage us to use the dependence of $R_{3/2}$ on Q^2 to determine the strong coulping constant α_s.

References

1. S. Catani, Y. L. Dokshitzer, M. H. Seymour and B. R. Webber, Nucl. Phys. B **406** (1993) 187.
2. K. H. Streng, T. F. Walsh and P. M. Zerwas, Z. Phys. C **2** (1979) 237.
3. Z. Nagy and Z. Trocsanyi, Phys. Rev. Lett. **87**, 082001 (2001)
4. J. Pumplin, D. R. Stump, J. Huston, H. L. Lai, P. Nadolsky and W. K. Tung, JHEP **0207**, 012 (2002)
5. H. L. Lai *et al.*, Phys. Rev. D **55**, 1280 (1997)
6. A. D. Martin, R. G. Roberts, W. J. Stirling and R. S. Thorne, Eur. Phys. J. C **28** (2003) 455
7. S. Catani and M. H. Seymour, Nucl. Phys. B **485** (1997) 291

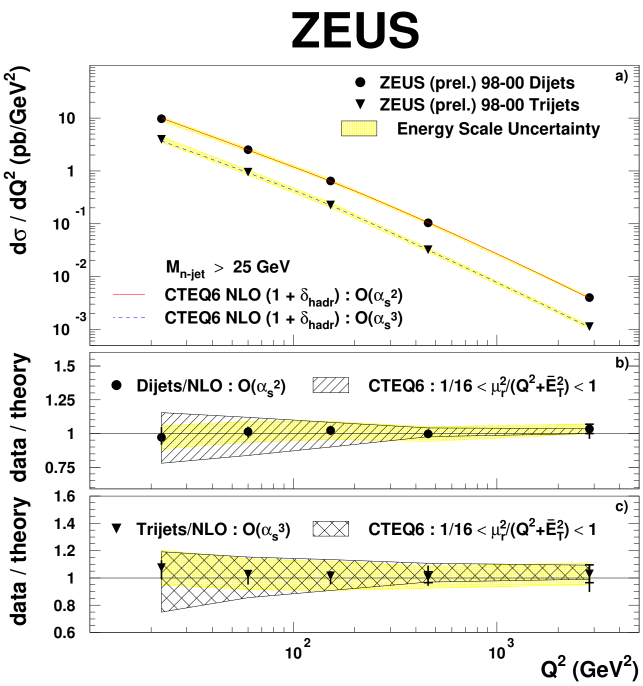

Figure 1. a) The inclusive dijet and trijet cross sections as functions of Q^2. The inner error bars represent the statistical uncertainties and the outer error bars represent the quadratic sum of all uncertainties. The shaded band indicates the calorimeter energy scale uncertainty. The predictions of perturbative QCD in next-to-leading order with CTEQ6 PDF are compared to the data. b) and c) show the ratio of the data over predictions. The hatched band represents the renormalisation scale uncertainty of the QCD calculation.

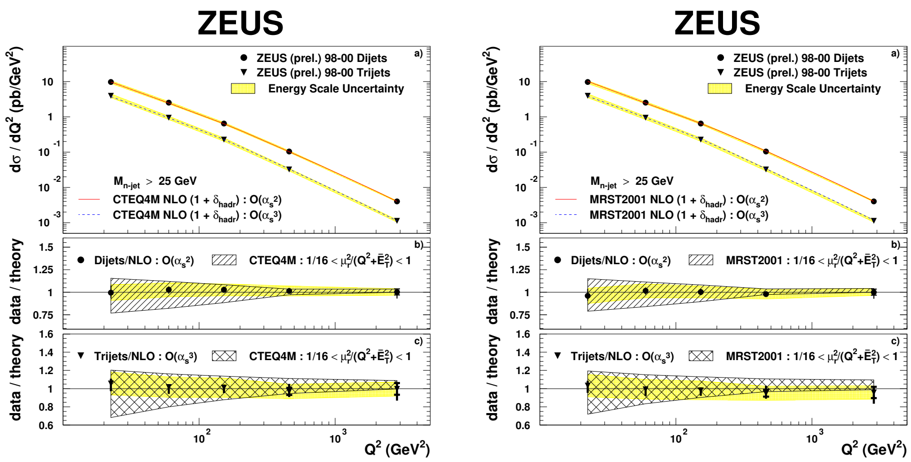

Figure 2. a) The inclusive dijet and trijet cross sections as functions of Q^2. The predictions of perturbative QCD in next-to-leading order with CTEQ4M (*left*) and MRST2001 (*right*) PDF are compared to the data. Other details are as described in the caption in Fig. 1.

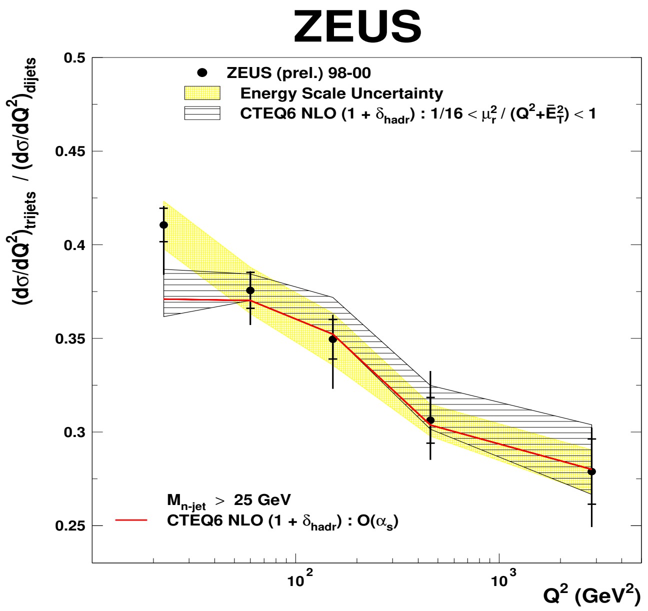

Figure 3. The ratio of inclusive trijet over dijet cross section as a function of Q^2. The predictions of perturbative QCD in next-to-leading order with CTEQ6 PDF are compared to the data. Other details are as described in the caption in Fig. 1.

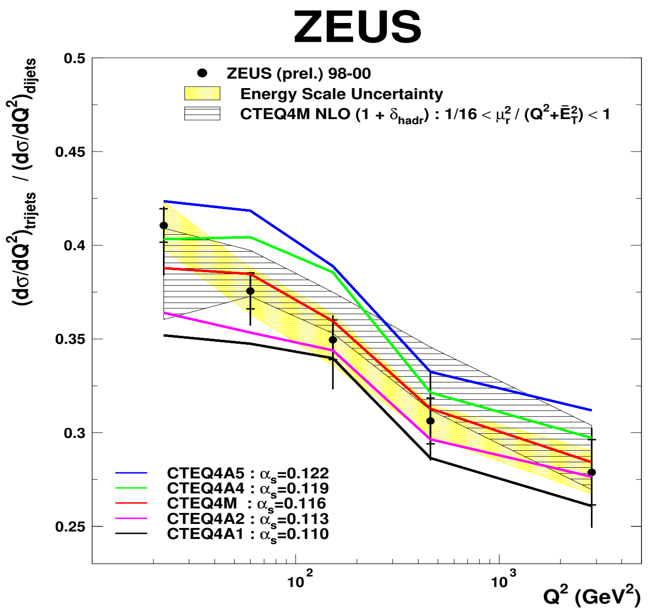

Figure 4. The ratio of inclusive trijet over dijet cross section as a function of Q^2. The predictions of perturbative QCD in next-to-leading order with five sets of the CTEQ4 PDF are compared to the data. Other details are as described in the caption in Fig. 1.